JOURNAL OF PROPULSION AND POWER
Vol. 20, No. 3, May–June 2004

Static Control of Combustion Oscillations by Coaxial Flows: A Large-Eddy-Simulations Investigation

J. U. Schlüter*
Stanford University, Stanford, California 94305-3030

In the design process of lean premixed combustors, the suppression of combustion instabilities plays a crucial role. Because active control measures to suppress combustion instabilities involve costs and maintenance, passive or static control measures are a preferable choice. The current work focuses on vortex-driven combustion instabilities, where large-scale vortices trigger the instability. A skillful vortex management in the combustor by passive methods—such as a coaxial flow—should be able to decrease the influence of large-scale vortices on the flame or to suppress the creation of large vortices completely. The current study investigates the possibilities of manipulating the shear layer at the burner nozzle of an axisymmetric dump combustor by a small circumferential coaxial flow. To explore these possibilities of flow control, large eddy simulations (LES) of a confined Bunsen burner flame are performed using a flow solver based on a low-Mach-number assumption and the *G* equation. The flow is periodically excited in order to simulate the acoustic forcing of the combustion instability. Phase averaging delivers the flow response to the forcing, and transfer functions give information about the amplification of the forcing. The success of the control method is then determined by the ability of the control method to suppress an amplification of the periodic excitation. The results of LES of the cold flow shows that the swirled coaxial flow is able to destroy large-scale structures and to suppress the periodic flow response substantially. In the reacting case a coaxial flow is able to shield the main flow and the flame front from large-scale vortices, and the influence of vortices on the flame front decreases dramatically.

I. Motivation

A. Vortex-Driven Combustion Instabilities

THE control of combustion instabilities is crucial for the successful design of of lean premixed combustors. The susceptibility of of these combustors to combustion instabilities[1,2] makes it a delicate task to apply these kind of combustors to civil aircraft engines. The control of combustion instabilities is critical in order to progress towards highly efficient, low-pollutant combustors.

There are several mechanisms suspected of leading to combustion instabilities, such as periodic inhomogeneities in the mixture fraction, pressure sensitivity of the flame speed, and the formation of large-scale turbulent structures.[3–5] Although an attempt to suppress combustion instabilities in practical applications has to address all of these sources, the current work focuses on coherent structures as the driving mechanism in creating noise.

In vortex-driven combustion instabilities[6] the roll up of a coherent structure near the burner nozzle bundles an amount of unburned fresh gases inside and increases the flame surface dramatically (Fig. 1). As a result, the fresh gases burn rapidly at a very distinct moment. The sudden heat release creates an acoustic wave, which—given the proper time lag—delivers an acoustic perturbation. Because an acoustic perturbation triggers the roll up of a coherent structure in the shear layer,[7–9] the next vortex is created near the edge of the burner nozzle.

The Rayleigh criterion can be used to determine whether this process is self-amplifying: if the sudden heat release is in phase with the acoustic wave creating the next inhomogeneity, then this cycle will be repeated with a certain frequency.

The consequences of unstable combustion are often troublesome because of the intense pressure-fluctuation levels that can occur, as well as increased heat transfer to the combustor surfaces.[4,10] These conditions can result in system performance degradation (for example, an increase in the lean blow-off limit or unsteadiness in thrust production in the case of a propulsion device), unacceptable vibration or noise levels, and, in the worst case, system failure because of structural damage.[2] The numerical prediction of combustion instabilities is challenging and has been tried with extensive simplifications.[11–13]

B. Active vs Static Control

So far, many control strategies for combustion instabilities are based on active-control mechanisms.[2] Active control is achieved by a sensor in the combustion chamber, which measures frequency and phase of a combustion oscillation. The measured signal is then analyzed, and a proper periodic response is determined. The response is either an acoustic perturbation or a modulation of the fuel supply.[14] Active control is able to suppress combustion instabilities substantially and is already in use for numerous practical applications, for example, in stationary industrial gas turbines for power generation.

However, this apparatus for active control is rather expensive and maintenance intensive. Furthermore because a failure of the active control system can lead to a failure of the whole combustion system this approach is not advisable for aircraft engines.

Static-control strategies built on fixed hardware installations in order to manipulate the characteristics of the flow in the combustor are more robust and need a minimum of maintenance. With static control a burner that is naturally less prone to combustion instabilities can be designed. However, to give design guidelines for static control measures this type of control has to be investigated in more detail.

C. Static-Control Strategies

Several static-control strategies for shear layers are known. The method that has received most attention is to use noncircular nozzle shapes like triangles[15,16] and ellipses.[17,18] However, the design of swirl combustors calls for axisymmetric nozzle shapes in order to generate swirl efficiently. Although swirl flames are not part of the current investigation, the ultimate goal of this study is to provide control strategies for swirl combustors.

Some control strategies involve hardware installations inside the shear layer. Honeycombs have had success in straightening the flow and destroying coherent structures efficiently.[19] The installation of these devices in practical burners is rather difficult because they

Received 3 December 2002; revision received 28 July 2003; accepted for publication 29 July 2003.

*Research Associate, Center for Turbulence Research. Member AIAA.

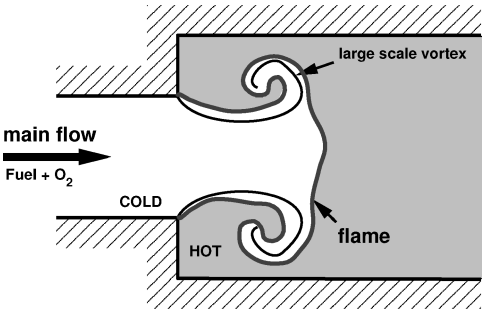

Fig. 1 Sketch of coherent structures as the driving mechanism in combustion instabilities.

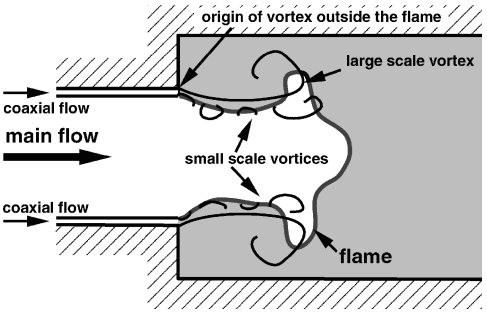

Fig. 2 Static control by coaxial flow: The origin of large-scale vortices is displaced outside the flame.

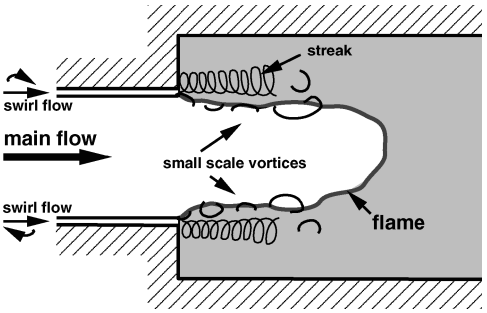

Fig. 3 Static control by swirled coaxial flow: the generation of longitudinal streaks destroys large-scale structures and enhances small-scale mixing.

would have to be placed into the flame front. The excessive heat these devices would have to sustain makes the application of these installations unlikely.

One possibility of altering the nature of the shear layer fundamentally is to use a small slit near the edge at the backward-facing side of burner edge. Suction is a very efficient way to deflect the flow and to avoid large-scale structures.[20] However, in a premixed burner it could mean that fresh cold gases at a temperature close to the ignition point are part of the fluid sucked out of the combustion chamber. The further treatment of these gases is problematic.

The current study investigates static control in the form of a small circumferential slit around the nozzle, blowing a coaxial flow into the combustion chamber. This coaxial flow carries less than 5% of the mass flow rate of the main flow and can be used in two ways to control coherent structures:

1) Displacement of the main shear layer (Fig. 2) is the first way: the shear layer between the coaxial flow and the recirculation zone creates large-scale vortices, while the shear layer between main flow carrying the fresh gases and coaxial flow creates less intense vortices because the velocity difference is small. This displaces the origin of the large-scale vortices for a small amount in outward radial direction. Although the intensity of coherent structures is unchanged, their influence decreases because the origin of these vortices is now outside of the flame front.

2) The second way is three-dimensionality of the shear layer (Fig. 3): by giving the shear layer a component in the third direction, for example, by swirl, a second shear layer perpendicular to the main shear layer is created. As a result, a longitudinally oriented vortex streak is created, which disturbs vortex creation in the main shear layer.[20]

II. Static-Control Investigation

A. Numerical Tools for Turbulence Research

Recent progress in numerical tools provides new elements in turbulence research. Whereas flow solvers based on a Reynolds-averaged Navier–Stokes formulation can predict the main flow features, large-eddy simulations (LES) are able to provide a detailed look at the origin, development, and decay of large-scale turbulent structures. This allows a deeper insight into the dynamics that govern coherent structures and ultimately can deliver answers on how to control the flow.

The advantage of numerical investigations over experiments is that a single parameter can be varied, leaving all other flow parameters unchanged. Experimental investigations usually encounter practical difficulties in achieving this goal.

Because the current work focuses on coherent structures as an origin of combustion instabilities, LES can be seen as the optimal tool to to find strategies to control large-scale structures in order to suppress combustion instabilities.

B. Test Case

To obtain data about general ideas for static control, the current investigation examines a flow over an axisymmetric backward-facing step at a Reynolds-number $Re = 3 \times 10^4$ (Fig. 4). The expansion ratio is 1:2 leading to an area ratio of 1:4. This geometry corresponds to that used in an experimental investigation,[21,22] and extensive data sets by laser-Doppler-anemometry measurements for the cold flow are available. Because the measurements provide velocity profiles upstream of the expansion, a proper definition of the inflow boundary condition is possible.[23]

Although the experiments are carried out with both a nonswirling and a swirling flow, the LES computation focuses here on the nonswirled case, where vortex dynamics are better understood. The dynamics governing swirl flows are still controversial,[24,25] and it is difficult to identify origin and control of a vortex structure in these flows.

C. Strategy of the Investigation

Because of the variety of physical phenomena, which lead to combustion instabilities, it is difficult to examine naturally excited combustion instabilities by numerical investigations. In the current investigation, therefore, the flow is forced by a convective wave in order to simulate periodic excitation by the combustion instability. A shear layer reacting to the periodic excitation amplifies the periodic disturbance. The quality of a static-control mechanism can be determined by the ability of the control mechanism to suppress the amplification of the excitation.

The external excitation of the flow makes it possible to assess the potential of a flame to create combustion instabilities by determining the transfer function of a combustor. Whether a flame is finally unstable or not depends on the ability of the heat release to create a periodic excitation that satisfies the Rayleigh criterion.

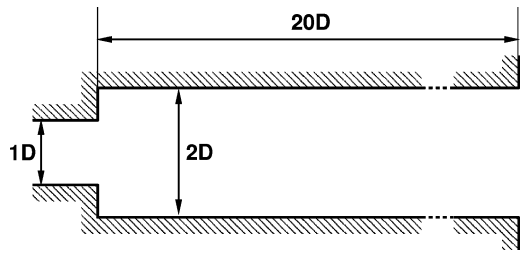

Fig. 4 Geometry of the combustor.

The prediction of this feedback mechanism is tedious because it involves computation of the acoustic wave propagation and knowledge of acoustic impedances at the boundaries of the computational domain. Here, for simplicity, acoustic effects have been explicitly excluded by using a flow solver based on a low-Mach-number approximation. This makes it possible to have a detailed look at the one-way coupling between excitation and flame response. If static control results in a reduction of the flame response to the excitation over a broad frequency range, a decrease of the ability of the flame to create an acoustic perturbation can be demonstrated, indicating a robustness against combustion instabilities.

To quantify the effect of a static-control device, the following procedure is employed.

First, the cold flow is examined. An LES computation of the test case is compared to the experimental data to give an estimate of the accuracy of the applied approach.

Then, the excitation is carried out on the cold flow by a periodic modulation of the inlet profile. The shedding of coherent structures at the burner nozzle will lock into the forcing frequency, and a so-called triple decomposition can be applied to the flow variables.[26] The instantaneous variable consists of three components: the time-independent component, the coherent (periodic) component, and the incoherent turbulence:

$$f(x,t) = \underbrace{\bar{f}(x) + \tilde{f}(x,\phi)}_{=\langle f\rangle(x,\phi)} + f_r'(x,t) \tag{1}$$

where $\bar{f}(x)$ is the time average of f, $\tilde{f}(x,\phi)$ the periodic component derived by phase averaging, and $f_r'(x,t)$ the stochastic turbulent component.

Because $\tilde{f}(x,\phi)$ contains all periodic information about the excited flow, the kinetic energy of the periodic fluctuation:

$$\mathcal{E}(x,\phi) = \tfrac{1}{2}[\tilde{u}(x,\phi)^2 + \tilde{v}(x,\phi)^2 + \tilde{w}(x,\phi)^2] \tag{2}$$

can be computed, and its integral over all periods and the flow domain

$$E_{\text{per}} = \int_V \int_0^{2\pi} \mathcal{E}(x,\phi)\,\mathrm{d}\phi\,\mathrm{d}V \tag{3}$$

delivers the response of the flow system to a certain frequency. By several repetitions of the computation with different forcing frequencies, a transfer function can be determined. This makes it possible to assess the susceptibility of the flow to excitation over a wide frequency range.

In the third step an LES computation of the cold flow with the static-control mechanism is performed. Again, several computations are made with different forcing frequencies, and a transfer function is determined. The comparison of the two transfer functions delivers the effectiveness of the static-control mechanism on cold flow turbulence.

The fourth and final step involves the computation of a reacting flowfield. Because of the high computational costs, only one exemplary frequency is examined. Here the flame response is given by the heat release

$$\langle \dot{Q}\rangle_{\text{periodic}} \simeq \frac{\partial Q}{\partial \Theta}(\tilde{T}) \tag{4}$$

with Θ the angle of the trigger frequency and $\tilde{Q}$ determined on the phase-averaged temperature field. The heat release is based on phased-averaged quantities in order to determine the value independent from the temporal filter size. Subtracting the mean value from $\langle \dot{Q}\rangle$ delivers the periodic fluctuation $\dot{Q}$. The integral of the rms value of the periodic fluctuation of the heat release delivers an overall value of the flame response:

$$\Psi = \int_V \int_0^{2\pi} \mathrm{rms}(\tilde{\dot{Q}})\,\mathrm{d}\phi\,\mathrm{d}V \tag{5}$$

Because the heat release has the greatest potential to create an acoustic wave, it gives a measure on whether the burner design is susceptible to create noise caused by a convective wave.

The comparison between uncontrolled and controlled flames and the comparison between reacting and nonreacting flows can deliver an answer on whether flame control via turbulence control is possible.

D. LES Flow Solver

For the current investigation the LES flow solver developed at the Center for Turbulence Research[22] has been used. The code solves the filtered momentum equations:

$$\frac{\partial \bar{\rho}\tilde{\boldsymbol{u}}}{\partial t} + \nabla\cdot(\bar{\rho}\tilde{\boldsymbol{u}}\tilde{\boldsymbol{u}}) = -\nabla\bar{P} + \nabla\cdot(\mu+\mu_t)\tilde{\tau} \tag{6}$$

with $\bar{\rho}$ the filtered density, $\tilde{\boldsymbol{u}} = \overline{\rho\boldsymbol{u}}/\bar{\rho}$ the Favre-filtered velocity vector, and $\bar{P}$ the pressure. A low-Mach-number assumption is used, which means that the density is not a property influenced by the flow, but entirely determined by the chemical reactions. As numerical method, a second-order finite volume scheme on a staggered grid is used.[27] The subgrid stresses are approximated with an eddy-viscosity approach, where the eddy viscosity is determined by a dynamic procedure.[28,29]

E. *G*-Equation Approach

In reacting cases the G-equation approach is used to simulate a premixed flame.[30–33] The G-equation approach is based on the assumption that the flame front is much smaller than the LES grid. Hence, it is treated as a discrete surface defined as the isosurface G_0 of the scalar field G. This isosurface is convected by the velocity field $\boldsymbol{u}$, while it propagates normal to itself with the laminar burning velocity s_L and is determined by

$$\rho\frac{\partial G}{\partial t} + \underbrace{\rho\boldsymbol{u}\cdot\nabla G}_{\text{Convection}} = \underbrace{\rho s_L|\nabla G|}_{\text{Propagation}} \tag{7}$$

In this equation the balance of diffusion and chemical reactions is represented by the laminar burning velocity. Because this quantity is only defined at the flame front, Eq. (7) is only valid at the flame front.

Applying an LES filter to Eq. (7) leads to

$$\bar{\rho}\frac{\partial \tilde{G}}{\partial t} + \bar{\rho}\tilde{\boldsymbol{u}}\cdot\nabla\tilde{G} = \bar{\rho}s_T|\nabla\tilde{G}| - \bar{\rho}D_t^G\tilde{\kappa}|\nabla\tilde{G}| \tag{8}$$

with s_T the turbulent burning velocity, D_t^G the turbulent diffusivity, and $\tilde{\kappa}$ a curvature term. These parameters have to be described by an LES model. In the current case a Bunsen burner flame has been assumed, using the same modeling approach as the LES computation of a similar flame.[31]

The modeling of a premixed flame with a G-equation approach is still a matter of investigations. Current research is focusing on validating the model and on extending the model to accommodate lifted flames, extinction, reignition, and wall effects. The proper description of all of these phenomena will be important to address combustion instabilities as a whole. For the current study however, the current version of the approach can be still be considered adequate. The reason for that is that the present study focuses on the flame response to large vortices. The influence of the large vortical motions on the flame front is mainly determined by the convective term on the left-hand side of Eq. (8), where no modeling takes place. Hence, the current approach can be considered sufficient to determine the effect of large-scale vortices on the flame front.

F. Geometry and Mesh

The geometry consists of an axisymmetric expansion (Fig. 4). The computational domain starts one diameter D upstream of the expansion, with D the diameter of the jet, and ends $10D$ downstream of

the expansion in a convective outflow condition. The inflow velocity is generated by an independent LES computation of a periodic pipe flow, which records the velocity components in the outflow plane and provides the data as inflow conditions.

The coaxial flow (Fig. 5) is blown into the combustion chamber between $1.06R$ and $1.12R$ at the backward-facing step, with $R = D/2$ the radius of the jet. The flow is assumed laminar in a parabolic shape. For a bulk velocity of the coaxial flow equal to the bulk velocity of the main jet, this results in a mass flux of the coaxial flow of 4% of the main jet in the nonreacting case.

The mesh consists of $384 \times 64 \times 64$ cells, adding up to 1.6M cells. It is refined in regions of high shear, especially around the control slit. Mesh distribution of the flow with and without slit is exactly the same, with the exception of the control slit itself.

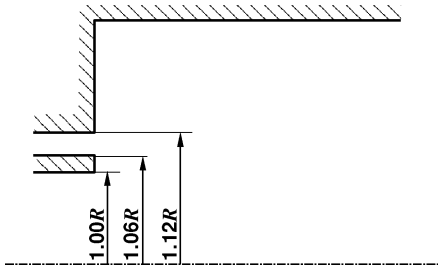

Fig. 5 Geometry of the coaxial jet (not to scale).

III. LES of the Cold Flow

A. Flow over an Axisymmetric Expansion

Because experimental data are available for the cold flow of the chosen test case, the first step is to validate the LES flow solver against the experiments. Figure 6 shows a comparison of LES and experiments of the mean axial velocity and the axial-velocity fluctuations. The mean axial-velocity component of the LES computation shows good agreement with the experiments, although the spreading rate of the shear layer behind the step is underestimated. The computed axial-velocity fluctuations also show good agreement with the experiment. However, the two profiles directly behind the step at $x/D = 0.5$ and 1.0 show some disagreements in shape. The highly turbulent nature of the flow in this region complicates measurements and computations alike.

B. Flow Response to Forcing

Forcing the flow triggers the roll up of coherent structures in the shear layer created by the main jet flow and the recirculation zone at the step. To determine the amplification of the forcing by the shear layer, the results of the LES computation are phase averaged. The phase averaging begins five periods after the flow forcing has been initiated to allow for adjustment to the periodic excitation. The averaging is then carried out over 30 periods. A separate study showed that this number of periods is sufficient to obtain a statistically converged phase average for the cold flow.

To visualize the vortex creation, Fig. 7a shows the the phase-averaged crosswise vorticity. The development of vortex rings

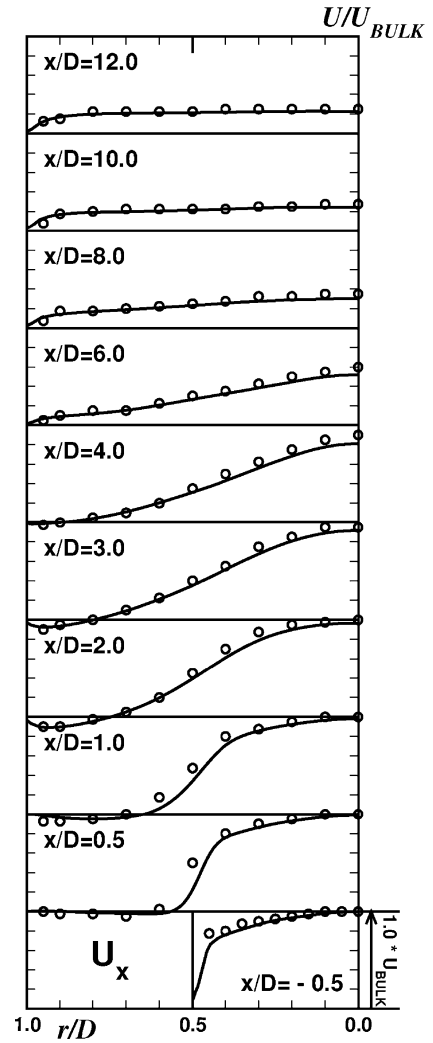

Fig. 6a Mean axial velocity component $\bar{u}_x$: ○, experimental data[22]; ——, LES of the cold flow.

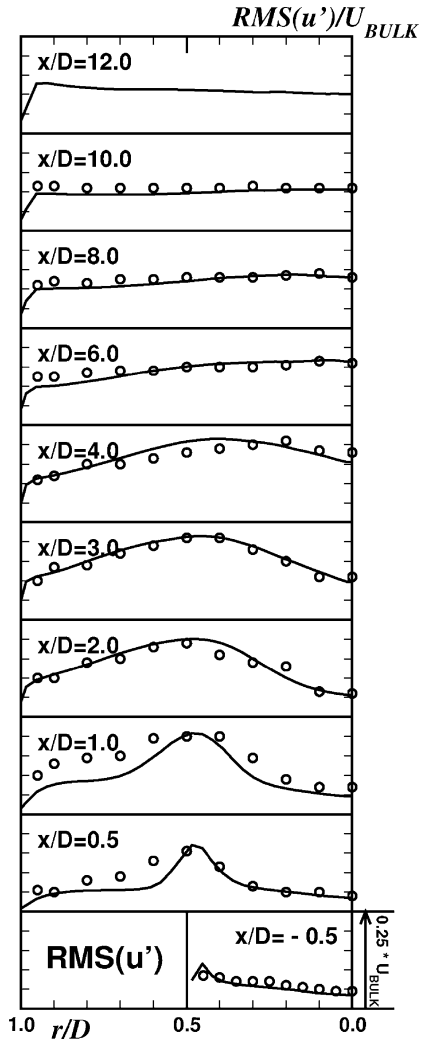

Fig. 6b Axial-velocity fluctuations $\sqrt{\overline{u_x'^2}}$: ○, experimental data[22]; ——, LES of the cold flow.

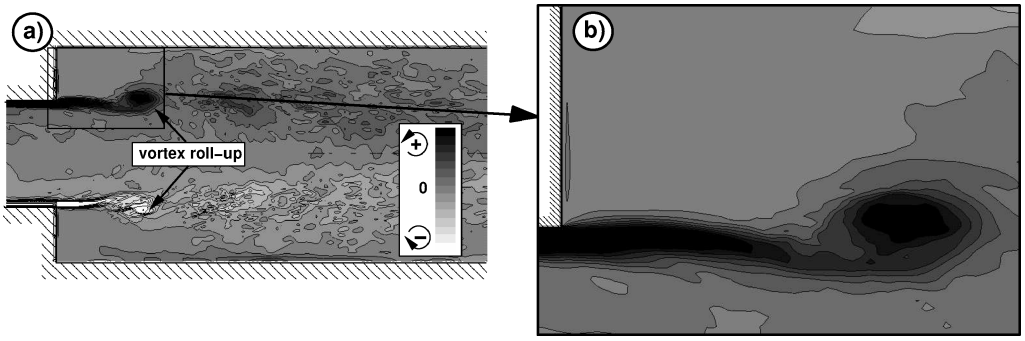

Fig. 7 Natural, uncontrolled vortex roll up (comp. Fig. 1). Nonreacting flow. Forcing frequency $Sr = 1.0$. Phase-averaged crosswise vorticity component $\tilde{\omega}_z$.

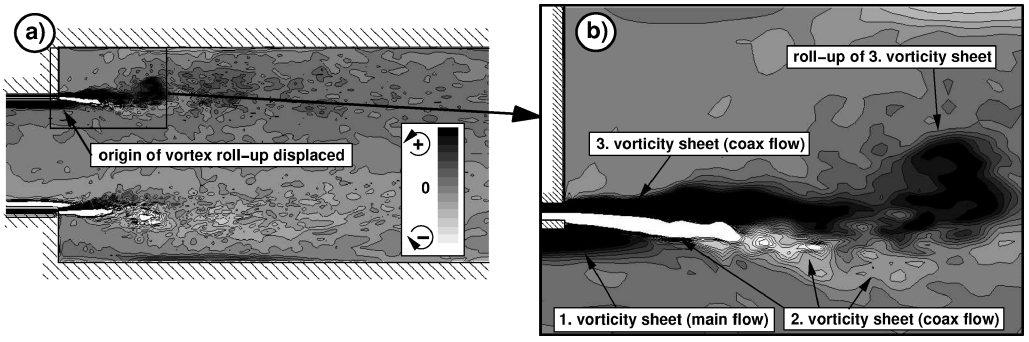

Fig. 8 Static control by high-speed coaxial flow ($u_{\text{coax}} = 2u_{\text{main}}$) (comp. Fig. 2). Nonreacting flow. Forcing frequency $Sr = 1.0$. Phase-averaged crosswise vorticity component $\tilde{\omega}_z$

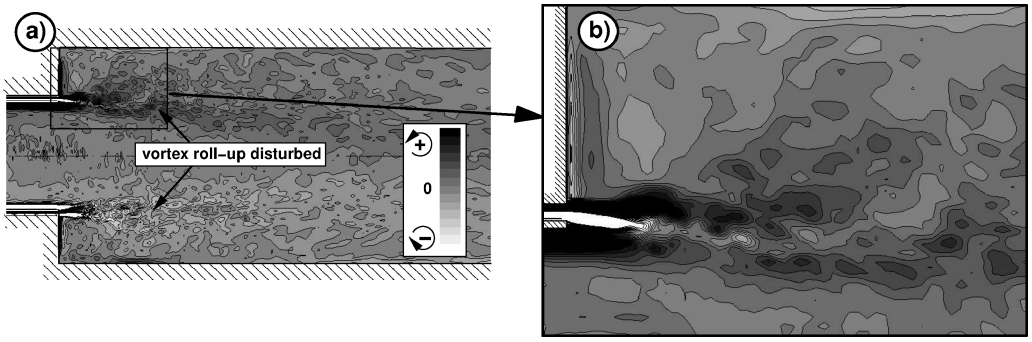

Fig. 9 Static control by swirled coaxial flow ($u_{\text{coax}} = 1 \cdot u_{\text{main}}$, swirl number $S = 0.25$, comp. Fig. 3). Nonreacting flow. Forcing frequency $Sr = 1.0$. Phase-averaged crosswise vorticity component $\tilde{\omega}_z$.

with the forcing frequency can be seen. Dark spots denote counterclockwise-turning eddies and light spots clockwise-turning eddies. A close-up of the upper part of the step (Fig. 7b) shows a vorticity sheet with positive sign (dark) created by the boundary layer and the shear layer between the main flow and the recirculation zone near the step. This vorticity sheet rolls up and creates the vortex ring. The static-control mechanisms aim to manipulate this vortex in order to control the flame.

The effect of a coaxial high-speed stream on the creation of a vortex ring can be seen in Fig. 8a. The coaxial flow, here with a bulk velocity twice as high as the main flow, creates two additional vortex sheets with opposite signs. The close-up in Fig. 8b shows how the vorticity sheet with negative sign (white) shields the main flow and restrains the vorticity sheet of the main flow from rolling up into a vortex. Instead, the outermost vorticity sheet originating in the coaxial flow rolls up. Because this vortex consists mainly of fluid emanating from the coaxial flow, it will have less influence on the flame front than in the uncontrolled case. However, the intensity of the vortex ring created by the coaxial flow is of approximately the same intensity as the vortex ring in the main flow in the uncontrolled case.

Figure 9a shows the employment of a swirled coaxial flow as a static-control mechanism. Here, the axial bulk velocity of the coaxial flow is the same as the bulk velocity of the main flow, and the swirl number

$$S = \frac{2}{R_i + R_o} \frac{\int_{R_i}^{R_o} r^2 \bar{u}_x \bar{u}_\phi \, \mathrm{d}r}{\int_{R_i}^{R_o} r \bar{u}_x^2 \, \mathrm{d}r} \tag{9}$$

is approximately $S = 0.25$, with u_x the axial velocity component, u_ϕ the azimuthal velocity component, R_i the inner radius of the coaxial slit, and R_o the outer radius of the coaxial slit. The swirl number of $S = 0.25$ was chosen arbitrarily. The effect of shielding the main flow by a vorticity sheet of opposite sign is still present (Fig. 9). Additionally, the creation of a shear layer in the azimuthal direction disturbs the vortex roll up of the coaxial flow, and a decrease of coherence in the vortex can be determined.

To quantify the effect of the control mechanisms, the kinetic energy of the periodic flow perturbation was computed and integrated over the volume behind the step. Figure 10 shows the results for different Strouhal numbers ($Sr = fD/U$, with f the forcing

frequency, D the diameter of the jet diameter, and U the bulk velocity of the jet.).

The natural, uncontrolled flow is denoted by circles. The maximum kinetic energy occurs near $Sr = 0.625$. Below that Strouhal number the vortices created by the forcing are very large and get increasingly disturbed by the proximity of the outer wall. For sufficiently low Strouhal numbers no coherent structures can be observed because the confinement of the jet impedes the creation of coherent structures larger than the step height.

With increasing Strouhal number the coherent structures shed at the step get smaller, and thus their contribution to the periodic fluctuation of the flow decreases. Above a Strouhal number of $Sr = 2.0$, the influence of these coherent structures onto the main flow is neglectable. A comparison with the literature shows that combustion instabilities in gas-turbine burners occur in the same frequency range as the amplification of periodic disturbances found here.[34,35]

The effect of the unswirled coaxial flow is not reflected in this presentation because the vortex development is not prevented, but only displaced. The kinetic energy of the coaxial flow with the same bulk velocity as the main flow $u_{\text{coax}} = u_{\text{main}}$ is identical with the kinetic energy of the uncontrolled flow (crosses in Fig. 10). A high-speed coaxial flow ($u_{\text{coax}} = 2 \cdot u_{\text{main}}$) even amplifies the flow response (stars in Fig. 10) because the velocity difference in the outer shear layer between the coaxial flow and the recirculation zone is even higher than in the uncontrolled flow.

Because the goal of this control measure is not to prevent a vortex roll up, but to displace the vortex roll-up out of the flame front, the strength of the vortical structure remains the same, and hence the kinetic energy of the coherent structures is nearly constant. The effectiveness of this control measure has to be shown in reacting computations.

However, using a swirled coaxial flow shows great potential even in the cold flow. Even the low swirl number $S = 0.25$ results in a considerable damping of the flow response (triangles in Fig. 10). An increase of the swirl number decreases the flow response even more (squares in Fig. 10). Here it can be seen that the swirled coaxial flow is able to damp the flow response by more than 50% over a broad frequency range.

IV. LES of the Reacting Flow

A. Setup for Reacting Flow Computations

Because the computation of reacting flows is much more expensive, the determination of a transfer function for the reacting flow comparable to Fig. 10 is too costly to perform. Instead, a single forcing frequency is chosen, and several cases of coaxial flows are investigated and compared to the uncontrolled case. As a forcing frequency, the Strouhal number of $Sr = 1.0$ was chosen. This choice was made because the flow response for this frequency is still high, but the length of a period of this frequency is quite short, which allows the computation of a higher number of periods in the same computed physical time span.

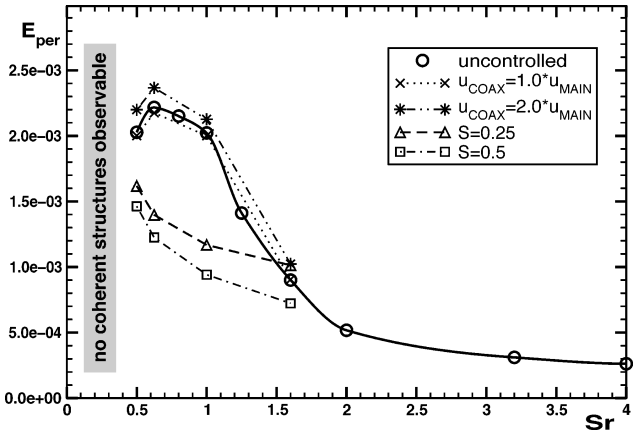

Fig. 10 Kinetic energy E_{per} of the periodic perturbation [see Eq. (3)] for different Strouhal numbers $Sr = f \cdot D/U$. The confinement of the jet impedes the creation of very large structures ($Sr < 0.5$).

In a reacting flow the coaxial flow can carry either fresh air or hot products. The injection of fresh air near the stabilization point of the flame would alter the chemical characteristics of the flame in comparison to the uncontrolled flow creating a liftoff of the flame. It would be difficult to assign the altered flame response of the burner modification to the liftoff or the manipulation of the large-scale vortical structures. Because the current investigation concentrates on the attempt to control a flame mechanically and not chemically, the coaxial flow in the computation carries hot products in order to provide the same chemical characteristics as the uncontrolled flame stabilized by the recirculation zone at the dump. Even though in practical applications it might be difficult to feed the coaxial flow with hot gases, for the current study it allows the variation of only a single parameter and the assignment of the effect of the coaxial flow to the vortex development and not altered chemical properties.

However, the choice of using hot products for the coaxial flow creates problems in investigating swirled coaxial flows. Because of the low density of the hot products, the swirl flow does not possess enough azimuthal momentum to influence the main jet. An increase of the azimuthal velocity component to compensate the momentum loss produced very high swirl numbers resulting in a fast decay of swirl. Hence, the investigation of swirled coaxial flows has to be left for future investigations, when a cold swirled coaxial flow can be employed and the liftoff of the flame can be part of the investigation.

B. Results of the Reacting Flow Computations

The instantaneous flame response to the forcing of the inflow can be assessed by a look on the temperature distribution in the combustor. Figure 11 shows an instantaneous snapshot of the uncontrolled periodically excited flow. The influence of the vortices created by the forcing can be seen in different stages. In the beginning the vortices bulge the flame front. Fully developed, the vortices create the typical mushroom-shaped distortion of the flame, and during their decay the vortices finally detach parts of the flame. These flame pockets float far downstream, where they are consumed.

Figure 12 shows the same flame with a low-speed coaxial flow. Large-scale vortices still distort the flame front, but have much less influence because they are created outside the flame. Comparing Figs. 11 and 12, the most striking difference is that the flame with static control is more compact and seems much steadier than its uncontrolled counterpart, and no flame detachments take place. Because the small-scale mixing is enhanced by the coaxial flow, the flame length in this combustor is shorter than in the case without coaxial flow.

Using a high-speed coaxial flow (Fig. 13), the effect of the vortex rings on the flame decreases even more. Even though large-scale vortices are created, which have a higher kinetic energy than in the uncontrolled case, the origin of these vortices is a little displaced in outward radial direction. Although this displacement is very small, it is sufficient to decrease the influence of this vortex to the flame front.

Because both flames using a coaxial flow have the same total heat release as the uncontrolled flame, but are able to burn all fresh gases on a shorter length scale, the flames with a coaxial flow are more efficient than their uncontrolled counterpart.

To give a quantitative measure on the effectiveness of the control method, the flow was phase averaged, and the periodic heat release determined according to Eq. (5). Because the computational costs for reacting flows are high, not as many periods can be computed as in the cold flow. The actual value has to be approximated by the convergence history of the phase average (Fig. 14). Before starting the averaging, the flow has been excited for five periods in order to let the flow adjust to the new inlet conditions.

In the uncontrolled case the phase average converges after 16–18 periods of excitation. The erratic nature of the flame detachments results in highly stochastic turbulence, and as such, the phase-averaging process takes a large number of periods.

Using the coaxial flow to control the flame, the flame becomes more stable, and the averages start to converge earlier, already at 8–10 periods.

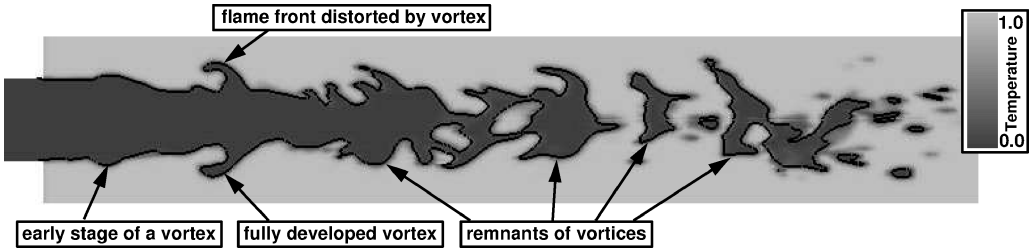

Fig. 11 Uncontrolled flame. Instantaneous snapshot after six periods of forcing. Forcing frequency $Sr = 1.0$: gray scale, temperature T; ——, G_0 (flame front).

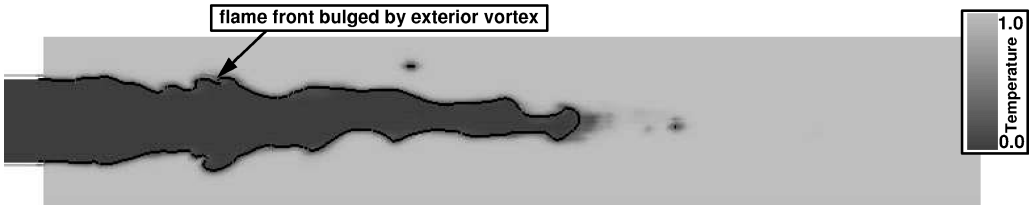

Fig. 12 Static control by low-speed coaxial flow ($u_{coax} = 1 \cdot u_{main}$). Instantaneous snapshot after six periods of forcing. Forcing frequency $Sr = 1.0$: gray scale, temperature T; ——, G_0 (flame front).

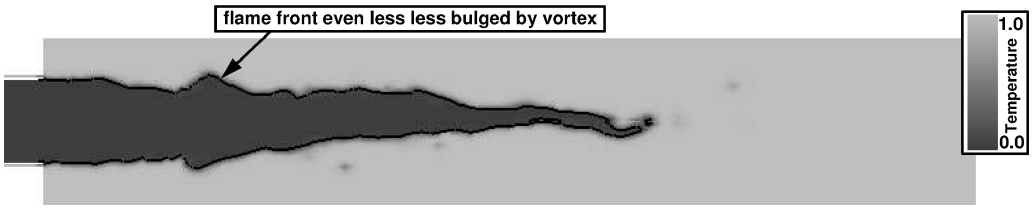

Fig. 13 Static control by high-speed coaxial flow ($u_{coax} = 2 \cdot u_{main}$). Instantaneous snapshot after six periods of forcing. Forcing frequency $Sr = 1.0$: gray scale, temperature T; ——, G_0 (flame front).

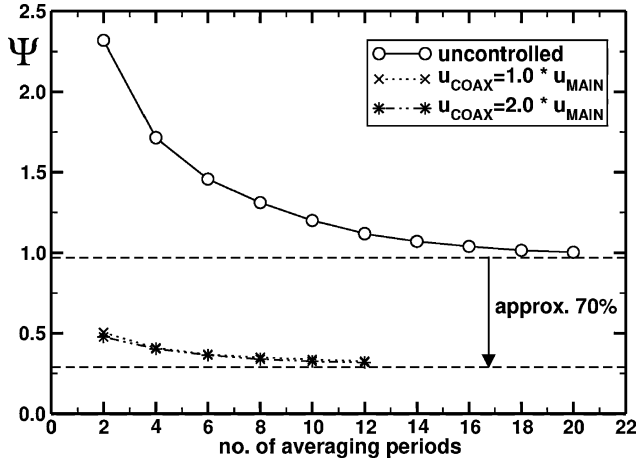

Fig. 14 Periodic heat release [see Eq. (5)] in dependency of the number of averaging periods. Strouhal number $Sr = \text{const} = 1.0$.

Even though the flow reacts less stochastic, the burner design with the coaxial flow responds to velocity oscillations with a periodic heat release approximately 70% below the uncontrolled case. That means that a velocity perturbation coming from upstream of the flame is much less amplified, and it is more likely that this burner does not fulfill the Rayleigh criterion. Hence, this burner design can be attested to be a robustness against combustion instabilities.

A similar procedure can be applied to compute the kinetic energy of the flow oscillations. Here, the static control results in a 60% reduction of the flow response.

V. Conclusions

LES has been used to examine the influence of large-scale vortices on combustion oscillations. The usage of a flow solver based on a low-Mach-number approximation made it possible to explicitly exclude acoustic effects and pressure sensitivity of the flame and to link the effects of the flame response directly to the forcing of the flow and the creation of large-scale vortices. LES has been shown to be a powerful tool in this investigation, because it was possible to vary parameters independent from others.

The here described static-control mechanism in the form of a coaxial flow has shown a large potential in suppressing combustion instabilities. The change of the burner design resulted in a dramatic decrease of the flame response to external excitations. This robustness of the burner design makes it less prone to combustion instabilities.

In contrast to active control, the proposed static control of the combustor requires a minimum of maintenance. The simplicity of this change makes it possible to use static control in order to replace or to support active-control efforts.

References

[1]Putnam, A. A., "Combustion Driven Oscillations in Industry," Elsevier, New York, 1971.

[2]McManus, K. R., Poinsot, T., and Candel, S. M., "A Review of Active Control of Combustion Instabilities," *Progress in Energy Combustion Science*, Vol. 19, Feb. 1993, pp. 1–29.

[3]Mugridge, B. D., "Combustion Driven Oscillations," *Journal of Sound and Vibration*, Vol. 70, June 1980, pp. 437–452.

[4]Büchner, H., Hirsch, C., and Leuckel, W., "Experimental Investigations on the Dynamics of Pulsated Premixed Axial Flames," *Combustion Science and Technology*, Vol. 94, No. 1, 1993, pp. 219–228.

[5]Peters, N., and Ludford, G. S. S., "The Effect of Pressure Variations on Premixed Flames," *Combustion Science and Technology*, Vol. 34, Dec. 1983, pp. 331–344.

[6]Poinsot, T. J., Trouvé, A., Veynante, D., Candel, S., and Esposito, E., "Vortex-Driven Acoustically Coupled Combustion Instabilities," *Journal of Fluid Mechanics*, Vol. 177, 1987, pp. 265–292.

[7]Crow, S. C., and Champagne, F. H., "Orderly Structure in Jet Turbulence," *Journal of Fluid Mechanics*, Vol. 48, No. 3, 1971, pp. 547–591.

[8]Ho, C. M., and Huang, L. S., "Subharmonics and Vortex Merging in Mixing Layers," *Journal of Fluid Mechanics*, Vol. 119, 1982, pp. 443–473.

[9]Ho, C., and Huerre, P., "Pertubed Free Shear Layers," *Annual Review of Fluid Mechanics*, Vol. 16, 1984, pp. 365–424.

[10]Lang, W., Poinsot, T., and Candel, S., "Active Control of Combustion Instability," *Combustion and Flame*, Vol. 70, Dec. 1987, pp. 281–289.

[11]Brookes, S. J., Cant, R. S., and Dowling, A. P., "Modeling Combustion Instabilities Using Computational Fluid Dynamics," American Society of Mechanical Engineers, Paper 99-GT-112, June 1999.

[12]Veynante, D., and Poinsot, T., "Large Eddy Simulation of Combustion Instabilities in Turbulent Premixed Burners," *Annual Research Briefs*, Center for Turbulence Research, Stanford, 1997, pp. 253–274.

[13]Angelberger, C., Veynante, D., and Egolfopoulos, F., "LES of Chemical and Acoustic Effects on Combustion Instabilities," *Flow Turbulence and Combustion*, Vol. 65, No. 2, 2000, pp. 205–222.

[14]Paschereit, C. O., Gutmark, E., and Weisenstein, W., "Control of Thermoacoustic Instabilities in a Premixed Combustor by Fuel Modulation," AIAA Paper 99-0711, Jan. 1999.

[15]Schadow, K. C., Gutmark, E., Parr, D. M., and Wilson, K. J., "Selective Control of Flow Coherence in Triangular Jets," *Experiments in Fluids*, Vol. 6, No. 2, 1988, pp. 129–135.

[16]Gutmark, E., Schadow, K. C., Parr, T. P., Hanson-Parr, D. M., and Wilson, K. J., "Noncircular Jets in Combustion Systems," *Experiments in Fluids*, Vol. 7, No. 4, 1989, pp. 248–258.

[17]Husain, H. S., and Hussain, A. K. M. F., "Controlled Excitation of Elliptic Jets," *Physics of Fluids*, Vol. 26, No. 10, 1983, pp. 2763–2765.

[18]Hussain, A. K. M. F., and Husain, H. S., "Passive and Active Control of Jet Turbulence," *Turbulence Management and Relaminarisation*, edited by H. W. Liepmann and R. Natasimha, Springer-Verlag, Berlin, 1987, pp. 445–457.

[19]Nieberle, R., "Entwicklung einer Methode der Mustererkennung zur Analyse Kohärenter Strukturen und ihre Anwendung im Turbulenten Freistrahl," *Fortschrittsberichte VDI*, Reihe 7, Strömungsmechanik(106), VDI Verlag, Aachen, Germany, 1986.

[20]Fiedler, H. E., "Control of Free Turbulent Shear Flows," *Flow Control*, edited by M. Gad-el-Hak, A. Pollard, and J. P. Bonnet, Springer-Verlag, Berlin Heidelberg, 1998, pp. 335–429.

[21]Dellenback, P. A., "Heat Transfer and Velocity Measurements in Turbulent Swirling Flows Through an Aprupt Axisymmetric Expansion," Ph.D. Dissertation, Arizona State Univ., Phoenix, AZ, Dec. 1986.

[22]Dellenback, P. A., Metzger, D. E., and Neitzel, G. P., "Measurements in Turbulent Swirling Flow Through an Aprupt Axisymmetric Expansion," *AIAA Journal*, Vol. 26, No. 6, 1988, pp. 669–681.

[23]Pierce, C., and Moin, P., "Large Eddy Simulation of a Confined Coaxial Jet with Swirl and Heat Release," AIAA Paper 98-2892, June 1998.

[24]Gupta, A. K., Lilley, D. G., and Syred, N., *Swirl Flows*, Energy and Engineering Science, Abacus Press, Kent, UK, 1984, Chap. 4.

[25]Keller, J. J., "On the Interpretation of Vortex Breakdown," *Physics of Fluids*, Vol. 7, No. 7, 1995, pp. 1695–1702.

[26]Hussain, A. K. M. F., "Coherent Structures—Reality and Myth," *Physics of Fluids*, Vol. 26, No. 10, 1983, pp. 2816–2849.

[27]Akselvoll, K., and Moin, P., "Large-Eddy Simulation of Turbulent Confined Coannular Jets," *Journal of Fluid Mechanics*, Vol. 315, 1996, pp. 387–411.

[28]Germano, M., Piomelli, U., Moin, P., and Cabot, W., "A Dynamic Subgrid-Scale Eddy Viscosity Model," *Physics of Fluids, A*, Vol. 3, No. 7, 1991, pp. 1760–1765.

[29]Moin, P., Squires, K., Cabot, W., and Lee, S., "A Dynamic Subgrid-Scale Model for Compressible Turbulence and Scalar Transport," *Physics of Fluids, A*, Vol. 3, No. 11, 1991, pp. 2746–2757.

[30]Williams, F. A., *Combustion Theory*, 2nd ed., Addison Wesley Longman, Reading, MA, 1985, Chap. 10.3.

[31]Duchamps de Lageneste, L., and Pitsch, H., "A Level-Set Approach to Large Eddy Simulation of Premixed Turbulent Combustion," *Stanford Annual Research Briefs*, Center for Turbulence Research, Stanford, 2000, pp. 105–116.

[32]Duchamps de Lageneste, L., and Pitsch, H., "Progress in Large-Eddy Simulation of Premixed and Partially Premixed Turbulent Combustion," *Stanford Annual Research Briefs*, Center for Turbulence Research, Stanford, 2001, pp. 97–107.

[33]Pitsch, H., and Duchamps de Lageneste, L., "Large Eddy Simulation of Premixed Turbulent Combustion Using a Level-Set Approach," *Proceedings of the Combustion Institute*, The Combustion Institute, Vol. 29, 2002, pp. 2001–2008.

[34]Paschereit, C. O., Gutmark, E., and Weisenstein, W., "Structure and Control of Thermoacoustic Instabilities in a Gas-Turbine Combustor," *Combustion Science and Technology*, Vol. 138, Sept. 1998, pp. 213–232.

[35]Schildmacher, K.-U., Koch, R., Krebs, W., Hoffmann, S., and Wittig, S., "Experimental Investigations of the Temporal Air-Fuel Fluctuations and Cold Flow Instabilities of a Premixing Gas Turbine Burner," American Society of Mechanical Engineers, Paper 2000-GT-84, May 2000.